Heliyon 9 (2023) e12950

Contents lists available at ScienceDirect

Heliyon

journal homepage: www.cell.com/heliyon

Research article

Leverage of weave pattern and composite thickness on dynamic mechanical analysis, water absorption and flammability response of bamboo fabric/epoxy composites

Gangadhar M. Kanaginahal [a], Suresh Hebbar [b], Kiran Shahapurkar [c,**], Mohammed A. Alamir [d], Vineet Tirth [e,f], Ibrahim M. Alarifi [g], Mika Sillanpaa [h,i,j,k], H.C.Ananda Murthy [l,m,*]

[a] Department of Mechanical Engineering, Jain College of Engineering and Research, Belgaum, 590008, India
[b] Department of Mechanical Engineering, National Institute of Technology Karnataka Surathkal, Mangalore, 575025, India
[c] Department of Mechanical Engineering, School of Mechanical, Chemical and Materials Engineering, Adama Science and Technology University, Adama, 1888, Ethiopia
[d] Department of Mechanical Engineering, College of Engineering, Jazan University, Jazan, 45142, Saudi Arabia
[e] Mechanical Engineering Department, College of Engineering, King Khalid University, Abha, 61411, Asir, Saudi Arabia
[f] Research Center for Advanced Materials Science (RCAMS), King Khalid University, Abha, 61413, P.O. Box No. 9004, Asir, Saudi Arabia
[g] Department of Mechanical and Industrial Engineering, College of Engineering, Majmaah University, Al-Majmaah, Riyadh, 11952, Saudi Arabia
[h] Department of Chemical Engineering, School of Mining, Metallurgy and Chemical Engineering, University of Johannesburg, P. O. Box 17011, Doornfontein, 2028, South Africa
[i] International Research Centre of Nanotechnology for Himalayan Sustainability (IRCNHS), Shoolini University, Solan, 173212, Himachal Pradesh, India
[j] Zhejiang Rongsheng Environmental Protection Paper Co. LTD, NO.588 East Zhennan Road, Pinghu Economic Development Zone, Zhejiang, 314213, PR China
[k] Department of Civil Engineering, University Centre for Research & Development, Chandigarh University, Gharuan, Mohali, Punjab, India
[l] Department of Applied Chemistry, School of Applied, Natural Science, Adama Science and Technology University, P O Box 1888, Adama, Ethiopia
[m] Department of Prosthodontics, Saveetha Dental College & Hospital, Saveetha Institute of Medical and Technical Sciences (SIMAT), Saveetha University, Chennai, 600077, Tamil Nadu, India

ARTICLE INFO

Keywords:
Plain and twill bamboo
Phenalkamine bio-based hardener
Thermal analysis
Dynamic mechanical analysis
Water absorption and flammability

ABSTRACT

Spar caps, which cover 50% of the cost of windmill blades, were made of unidirectional and biaxial glass/carbon reinforcements of 600 gsm with thicknesses ranging from 100 to 150 mm for blades 70–80 m long. The significance of this study was to utilize an economical biodegradable material i.e bamboo fabric of 125 gsm to fabricate a lightweight composite and study its behavior for spar caps applications. The aim of this research was to investigate the effect of weave pattern and composite size at coupon level under thermal, dynamic, water absorption, and flammability conditions. Composites comprising 125 gsm plain and twill weave bamboo as reinforcements/AI 1041 Phenalkamine bio-based hardener with epoxy B-11 as matrix were tested. Thermo-Gravimetric Analysis revealed that the weave pattern and composite thickness had an effect on the rate of weight loss and sustenance until 450 °C. The pattern had an effect on the glass transition temperature, as seen by Differential Scanning Calorimetry. The weave pattern and size

* Corresponding author. Department of Prosthodontics, Saveetha Dental College & Hospital, Saveetha Institute of Medical and Technical Sciences (SIMAT), Saveetha University, Chennai, 600077, Tamil Nadu, India.
** Corresponding author.
E-mail addresses: kiranhs1588@astu.edu.et (K. Shahapurkar), anandkps350@gmail.com (H.C.Ananda Murthy).

https://doi.org/10.1016/j.heliyon.2023.e12950
Received 16 October 2022; Received in revised form 9 January 2023; Accepted 10 January 2023
Available online 14 January 2023

thickness had an effect on energy storage and dissipation, displaying the damping behavior in DMA. The weave pattern and size had an effect on the rate of water absorption, which saturated after a few hours. The wettability and thickness of composites hampered the burning rate, with 5.4 mm thickness resulting in a 30% decrease.

1. Introduction

The ease of extraction, availability, biodegradability, mechanical and chemical properties of natural fibers have defined their selection for domestic applications. Natural Fiber Reinforced Composites have found importance in applications such as automobile parts, sports equipment, bicycles, aircraft cabin parts, packaging, and many more [1]. Challenges such as thermal stability, durability, resistance to water/moisture absorption, and so on, have hindered their full-fledged functionality and performance in high-end applications [2]. Research works have been focused on addressing these challenges by methods such as fiber treatments, fabric weave patterns, coatings, usage of additives, nano-materials, and so on [3]. The current trend of research works has been oriented towards weight reduction, processing materials out of bio-degradable waste, and manufacturing domestic materials such as roofs, hollow designed window frames, geotextile nets, etc [4]. Among the vast classification of natural fibers, bamboo has been widely chosen as a suitable reinforcement because it has shown a better stiffness/mass ratio than steel and aluminum. Testing of bamboo as reinforcement in form of strips, fibers, and mats have shown acceptable results for structural concrete components [5] and repeated load-bearing components [6]. As bamboo is naturally extracted in the form of fibers, they are addressed as pure bamboo and chemically, as viscose fibers [7,8]. By resisting wind and its own weight naturally, it has displayed bending and compressive strength [9]. In-depth study of a fiber structure and morphology such as the cellulose percentage, micro-fibrillar angle and crystallinity index of extracted fibers have shown an effect on mechanical properties [10,11]. Acetylated bamboo showed less water absorption and thermal degradation, whereas alkaline-treated bamboo displayed a higher crystallinity index, tensile strength and modulus [12]. Thermal studies showed degradation of bamboo strips at 310 °C due to loss of cellulose, at 471 °C due to lignin and no Glass transition temperature (T_g) [13]. Fiber diameter and hygrothermal conditions had an effect on the mechanical properties of bamboo/epoxy [14]. Similarly, 4% alkaline treated bamboo/epoxy showed higher mechanical and thermal properties [15]. A 5% Sodium Hydroxide (NaOH) treated bamboo/epoxy showed better tensile properties [16]. Dynamic Mechanical Analysis (DMA) indicated the T_g of the composite increased by the addition of NaOH treated bamboo to cardanol, but its thermal stability reduced as analyzed from Thermal Gravimetric Analysis (TGA) [17]. TGA analysis inferred addition of bamboo reduced the degradation temperature of Bamboo/Polyamide and modulus increased as determined from DMA [18]. The T_g of epoxy as observed from Differential Scanning Calorimeter (DSC) and DMA tests got reduced by addition of bamboo whereas an improvement in the thermal stability of bamboo/epoxy was determined from TGA [19]. Alkaline treatment of bamboo enhanced the tensile strength and also the T_g of bamboo/PLA as observed in DSC, whereas its Melting Temperature (T_m) got reduced. TGA showed a reduction in thermal resistance for treated bamboo/PLA [20]. A 4% alkaline treated bamboo/PLA showed better tensile properties at 40 wt% and T_g at 50 wt% [21]. At 60 wt%, short bamboo/PLA displayed higher flexural modulus, storage modulus, and creep resistance [22]. The damping properties were at peak when the addition of Calcium Carbonate ($CaCO_3$) treated bamboo was at 30 wt% in High Density PolyEthylene (HDPE). The DSC and X-Ray Diffraction (XRD) graphs showed an increase in crystallinity of extruded parts for treated bamboo [23]. The affinity of uni-directional bamboo/PolyEster (PE) for water absorption was higher compared to random-oriented bamboo/PolyPropylene (PP) [24]. DMA studies indicated kenaf/epoxy had better damping properties than bamboo/epoxy [25]. Similarly, 10:40 bamboo/kenaf/epoxy showed better tensile and impact strength [26]. Flexural properties of Hemp/bio-resin were better than bamboo/bio-resin with a better T_g and lower water intake [27]. The addition of silane-treated bamboo increased the thermal stability of epoxy [28]. The addition of bamboo increased the fire resistance of bamboo-glass/PP. Better thermal resistance and damping properties were observed for hybrid composites from TGA and DMA [29]. Few works conducted on studying the influence of composite thickness subjected to static and fatigue conditions, have shown a decrease in failure probability, an increase in defects, a decrease in fatigue life, and variation in curing of composites through the thickness [30,31]. The basalt plain weave fabrics indicated better tensile and compressive strength than twill weave due to higher interlacing density and binding effect between fibers [32]. The plain weave of kenaf and banana fibers displayed higher tensile strength than twill weave due to interlacing of fibers in both directions [33]. Tough the tensile strength of basket weave pattern was higher, its failure to strain was lower than plain weave pattern fabric [34]. As the spar caps of thick sections cannot be tested at coupon level, specimens between 1 and 5 mm thickness can be studied by taking into account the scaling effects [35].

The literature review provides insight into the research efforts that were exclusively focused on the weave pattern or the size influence on composite performance. According to the literature, little study has been conducted on the use of lightweight composites for spar cap applications and understanding the cumulative influence of weave pattern and size on composite behavior. Previous work on the material characterization and static investigations concluded that the weave pattern and thickness played a role in determining the performance of the composite [36]. Thus, the current work focuses on utilizing a biodegradable material of 125 gsm as reinforcement in the composite for the application. The secondary tests were conducted to determine the influence of weave pattern (plain and twill) and composite thickness (3.1, 4.3, 5.4 mm) of bamboo/epoxy-phenalkamine on composite behavior at higher temperatures and its ability to resist the flame spread, visco-elastic properties and affinity towards water absorption.

2. Experiment details

2.1. Fabrication of composites

To fabricate a lightweight composite, the raw materials used were as mentioned in Table 1. Here, 125 gsm plain and twill weave patterned reinforcement fabrics were processed by wet layup method. 5 sheets of fabric were piled with epoxy-phenalkamine resin to achieve 3.1 mm thickness. Similarly, 7 sheets of fabric were piled for 4.3 mm thickness and 9 sheets of fabric for 5.4 mm thickness. The epoxy resin and the hardener were mixed in a volumetric ratio of 1:1 and stirred at a pace. Achieving a uniform mixing was challenging as the densities of epoxy and hardener were different. The fabrics were wetted by the matrix using a metal pad till the respective thickness and were kept under a uniform load for 24 h. The different thickness composites obtained have been mentioned in Table 2. The density of composites obtained was 1.15 g/cm^3.

2.2. Thermal-gravimetric analysis (TGA)

Three samples of Plain weave composites (PWC) and Twill weave composites (TWC) of varying thickness were prepared in form of flakes and tested in Perkin Elmer TGA4000, Ricmond, California, USA, by subjecting to a temperature range from 25 °C to 700 °C. The heating rate was maintained at 10 °C/min and nitrogen atmosphere at 50 mL/min.

2.3. Differential Scanning Calorimeter (DSC)

In present work samples have been prepared in form of small flakes as the pan used for testing is about 2–3 mm. The fabrics from plain and twill weave were cut into small flakes and were packed in an air tight bag as three different samples. PWC and TWC composites of 3.1, 4.3 and 5.4 mm thickness were cut along the surface to get samples in flakes form. The samples were further tested on Perkin Elmer DSC6000 instrument, at KONSPEC Mangalore, by subjecting them to temperature from 25 °C to 400 °C. Heating was maintained at 10 °C/min. Nitrogen atmosphere was maintained at 50 mL/min.

2.4. Dynamic mechanical analysis (DMA)

Three samples of plain and twill weave composite with specimen size 55 mm × 13 mm × thickness were tested in TA InstrumentsQ800 (New Castle, DE, USA), as per ASTM D5418-01 by mounting on a dual-cantilever beam testing machine as shown in Fig. 1 (a-f). The amplitude was set at 10 μm and 1 Hz frequency. The heating rate was set at 3 °C/min and the heating range was from 25 °C to 180 °C.

2.5. Water absorption

Five specimens of plain and twill weave composite of specimen size 76.2 mm × 25.4 mm × thickness was kept in salt water (S) and distilled water (D). The testing was performed as per ASTM D570-98 standard. The saltwater was collected from the Arabian Sea and specimens were placed in the solution as shown in Fig. 2 (a-b). The specimens were weighed before immersing in the water and the measurements were noted in weights i.e., grams (gms). The specimens were kept in both solutions as shown in Fig. 2 (c-d) and were measured after immersing for 2, 6, 12, 24, 48, 72, 96, 120, and 144 h.

2.6. Flammability

Three samples of specimen size 127 mm × 13 mm × thickness was subjected to flammability test as per UL-94HB horizontal standards on ATLAS HVUL2, equipment as shown in Fig. 3 (a-c). The specimen was marked at 25 mm and 100 mm, along the length. The flame was ignited from a burner inclined at 45° to the horizontal specimen as per the standard mentioned above. The burner was placed at a 2 mm distance below the sample tip marked at 25 mm end. The timer starts once the flame reaches the 25 mm mark and a reading was noted when it reaches 75 mm. The burning rate was calculated as per standard equation

$$V = \frac{60 * L}{t}$$

where V = burning rate in mm/min L = burned length in mm, t = time in seconds.

Table 1
Materials used and their properties.

Material	Properties
Bamboo Fabric (Plain and Twill weave) was procured from Sreenath Weaving Industry, Rajasthan, INDIA	125 gsm, 2/30 × 2/30 yarn count
Epoxy Resin (B-11) was procured from Axotherm Industry, Peenya, Bengaluru, INDIA.	1.15–1.18 g/cm^3, 11,000–15,000 mPas @ 25 °C
Phenalkamine hardener (AI 1041) was procured from Axotherm Industry, Peenya, Bengaluru, INDIA.	0.98–1.0 g/cm^3, 20,000–50,000 mPas @ 25 °C

Table 2
Notation for composite thickness.

3P—3.1 mm thickness plain weave composite	3T—3.1 mm thickness twill weave composite
4P—4.3 mm thickness plain weave composite	4T–4.3 mm thickness twill weave composite
5P—5.4 mm thickness plain weave composite	5T–5.4 mm thickness twill weave composites

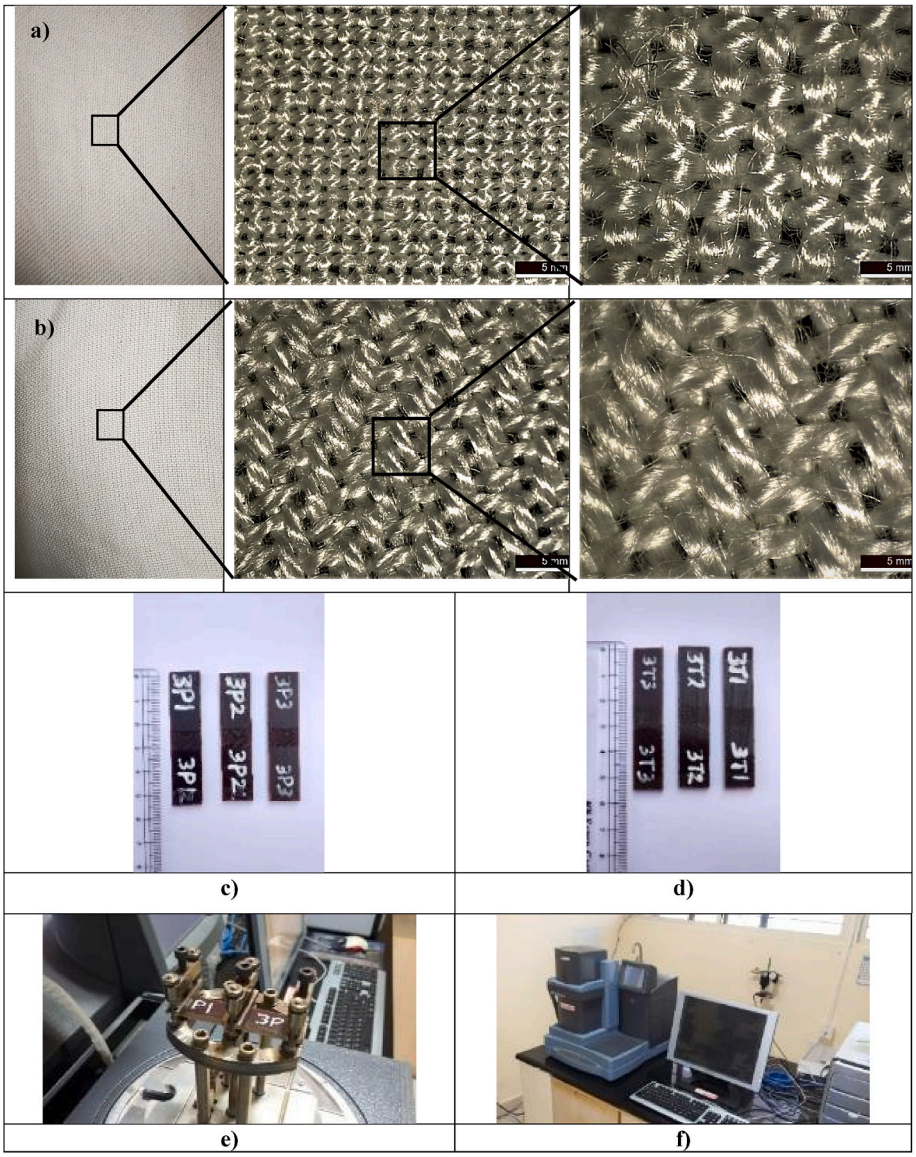

Fig. 1. a) Plain weave ||**b)** Twill weave and Dynamic testing (**c**) PWC, (**d**) TWC, (**e**)&(**f**) testing of samples at varying temperatures and constant frequency.

2.7. Scanning Electron Microscope (SEM)

Fractured specimens from DMA test were examined on Scanning Electron Microscope (SEM) - TESCAN VEGA3 AMU equipment at an operating voltage of 10 kV. The DMA tested specimens were coated with gold, by sputtering method and were kept in the equipment under vacuum for failure analysis. The failures were observed between 300X – 800X magnification to determine the failure.

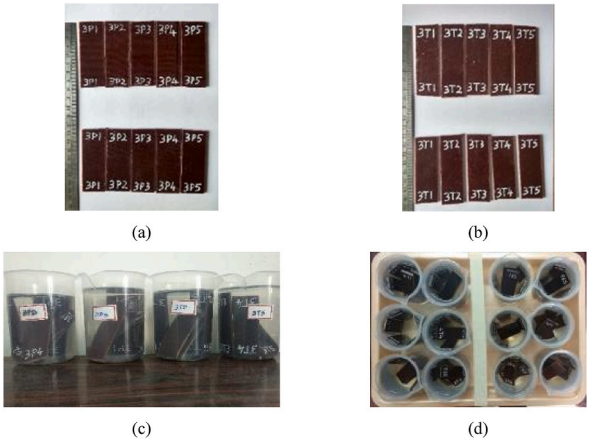

Fig. 2. Water absorption testing of (**a**) PWC, (**b**) TWC, (**c**)&(**d**) testing of samples in distilled and salt water solutions.

Fig. 3. Horizontal flammability testing of (**a**) PWC, (**b**) TWC & (**c**) testing of samples.

3. Results and discussion

The thermal degradation temperature, glass-transition temperature, and melting temperature observed from DSC and TGA are tabulated in Table 3, the burning rate results from flammability in Table 4 and percentage increase weight of PWC and TWC due to water absorption in Table 5.

3.1. Thermo-Gravimetric Analysis

In TGA the curve plotted in Fig. 4a, displays a 5% weight loss for the fabrics at 50 ± 5 °C and their respective composites at 255 ± 10 °C. The presence of the aromatic rings in the matrix produces the char residue, which acts as a protective coating and enhancing the initial degradation temperature (IDT) of PWC and TWC by 50% compared to their respective fabrics as observed in Table 3 [37,38,39]. The DTG curve plotted in Fig. 4b, displayed a lower rate of mass loss for TWC compared to PWC and their fabrics, inferring a better bonding at the interface. A larger mass of fabrics becomes degraded at 350 °C, whereas their respective composites sustain till 450 °C due to the matrix which acts as a coating [40,41,42]. The results indicated that though the weight loss of composites occurred at temperatures prior to pure resin, the derivate weight of composites showed sustainability till 450 °C compared to that of pure resin.

Table 3
TGA and DSC results of composites.

Sample	TGA			Var	DSC	Var
	$T_{5\%}$ (°C)	T_{max} (°C)	% Char @ 650		T_g (°C)	
Plain	46	332	1.776	1	–	
Twill	54	347	1.049	1.4	–	
3P	255	424	10.51	1.4	84.12	2
4P	256	427	10.73	1	83.56	2.4
5P	262	432	10.81	1.4	84.21	2.4
3T	251	436	11.88	1.4	88.48	2
4T	258	433	11.43	1	87.24	2
5T	262	434	11.08	1	87.72	2.4

TGA - Thermal Gravimetric Analysis, DSC - Differential Scanning Calorimeter, Var - Variance, $T_{5\%}$ - Temperature at 5% weight loss, T_g - Glass Transition Temperature, T_{max} - The temparture at maximum loss of weight.

Table 4
UL94HB flammability test results.

Sample	Seconds to Burn Damaged Length	Burning Rate (mm/min)	HB	Var
3P1	214.96	21.08	Pass	2.5
4P1	202.73	22.28	Pass	2
5P1	278.63	16.13	Pass	2.3
3T1	204.7	22.01	Pass	1.4
4T1	207.73	21.73	Pass	2.2
5T1	277.43	16.56	Pass	2.5

HB - Horizontal Burning.

Table 5
Percentage increase in Water absorption of PWC and TWC immersed in distilled (**D**) and salt water (**S**) solutions.

Composite Hours | Solution		3P	4P	5P	3T	4T	5T
2	D	0.24	0.22	0.16	0.21	0.14	0.13
	S	0.18	0.16	0.13	0.14	0.12	0.13
6	D	0.40	0.34	0.29	0.35	0.29	0.26
	S	0.33	0.28	0.24	0.29	0.24	0.23
12	D	0.65	0.55	0.45	0.57	0.45	0.41
	S	0.60	0.47	0.36	0.47	0.38	0.38
24	D	1.04	0.87	0.69	0.88	0.68	0.64
	S	0.97	0.74	0.58	0.71	0.60	0.57
48	D	1.57	1.31	1.04	1.25	1.00	0.95
	S	1.43	1.15	0.89	1.14	0.92	0.89
72	D	2.16	1.76	1.40	1.81	1.47	1.35
	S	2.00	1.58	1.23	1.57	1.29	1.22
96	D	2.81	2.29	1.82	2.36	1.92	1.77
	S	2.62	2.07	1.60	2.06	1.69	1.60
120	D	3.47	2.82	2.25	2.91	2.38	2.18
	S	3.25	2.56	1.98	2.55	2.09	1.98
144	D	4.13	3.35	2.67	3.46	2.84	2.60
	S	3.87	3.05	2.36	3.04	2.49	2.35

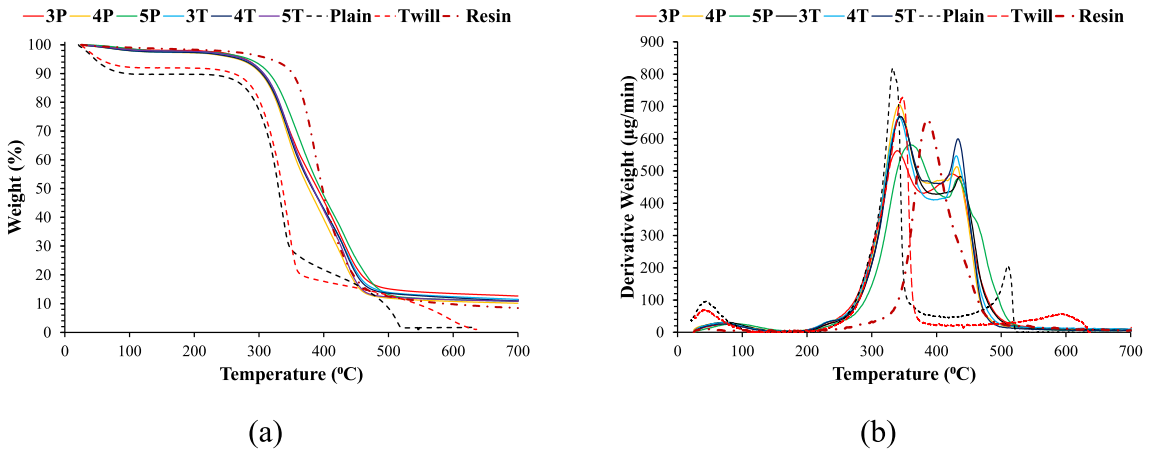

Fig. 4. (**a**) TG curve; (**b**) DTG curve.

3.2. Differential Scanning Calorimeter

An endothermic broad curve observed at 125 °C in Fig. 5a, indicates the loss of moisture, similar to the peaks observed in TG curves in Fig. 4a. An exothermic peak at 350 °C indicates the breakage of cellulose chains and pyrolysis of lignin, similar to peaks observed for DTG curves in Fig. 5b. The T_g values observed in Table 3 were 5% higher for TWC compared to PWC, indicating better curing and bonding with the matrix. The peaks observed at 370 °C were higher for 5T inferring maximum heat absorption capacity [43,44]. No exothermic peaks were observed below 150 °C/200 °C indicating a faster curing of PWC and TWC at room temperature [15].

The presence of hydroxyl groups observed in Fig. 6, indicated the existence of cellulose. This cellulose will bond with the matrix which indicates the aliphatic and aromatic chains, forming the interface which was observed by the shift in the peak of the hydroxyl

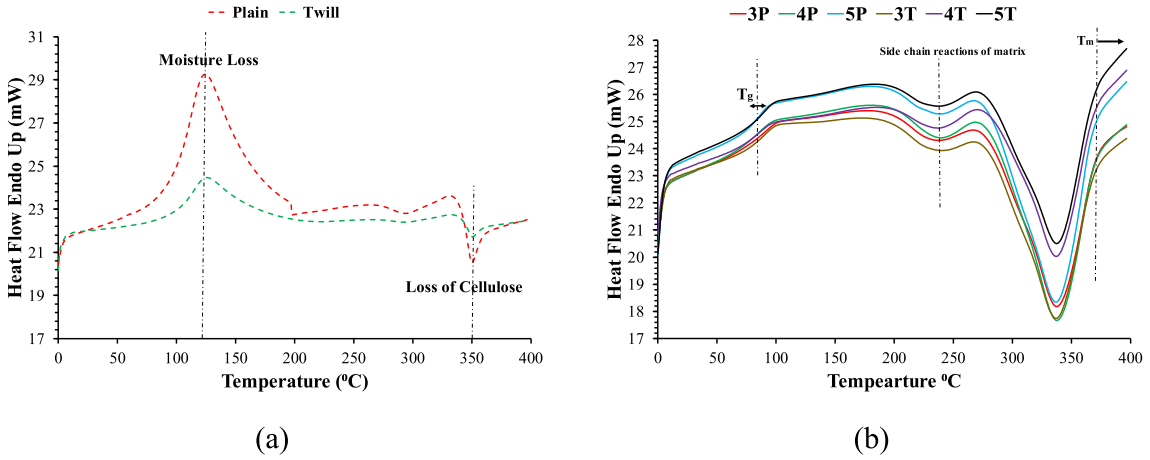

Fig. 5. (**a**) First heating of fabric; (**b**) Second heating of composites.

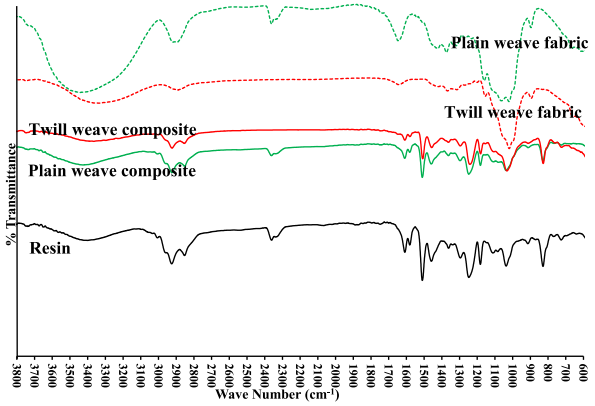

Fig. 6. FTIR analysis of fabric, resin, and composites [36].

group observed for the composites. Please refer to my previous work on characterization and structural analysis of composites for thorough information [36].

3.3. Dynamic mechanical analysis

Based on the observations made from TGA and DSC analysis, PWC and TWC composites were considered for further studies.

3.3.1. Storage modulus (E')

In the glassy region (<60 °C) as observed in Fig. 7a, 5T displayed higher E'compared to 5p, because of better wettability and fiber breakages observed from the micrographs in Fig. 8 [45]. With increasing temperature, the components in the glassy region break loose at the beginning of the T_g range as per micro-Brownian motion and with the relaxation of the amorphous phase, they co-ordinate large scale motions forming a steep slope in the transition region (>60 °C and <100 °C) [29]. Further increasing the temperature, the matrix softens and increases the free flow of components in rubbery region (>100 °C) [42]. In rubbery region the interfacial strength was determined from crosslinking density equation $\rho = \frac{E'}{\Phi RT}$ where ρ is crosslink density, Φ is front factor normalized to 1, R is gas constant and T is absolute temperature i.e., $T_g + 30$ °C [46]. The ρ calculated from the rubbery region as displayed in below Table 6, was higher for TWC than PWC.The E' of 5T showed 1.3 times that of 5P in rubbery region, indicating better stiffness [47]. Thus, 5T displayed better elastic and stiffness properties in glassy and rubbery regions.

3.3.2. Loss modulus (E'')

An unrecoverable energy dissipated in the form of heat due to the segmental motion of components at the interface results in E'' as plotted in Fig. 7b. PWC has shown an increase in T_g from 3P to 5P but their E'' values reduced, indicating a lower cross-linking density. Whereas TWC showed an increase in T_g and E'' from 3T to 5T, indicating a higher cross-linking density [48]. A 9% higher E'' displayed by 5T compared to 5P was due to better wettability observed from the micrographs in Fig. 8. It also indicated an increase in the ratio of

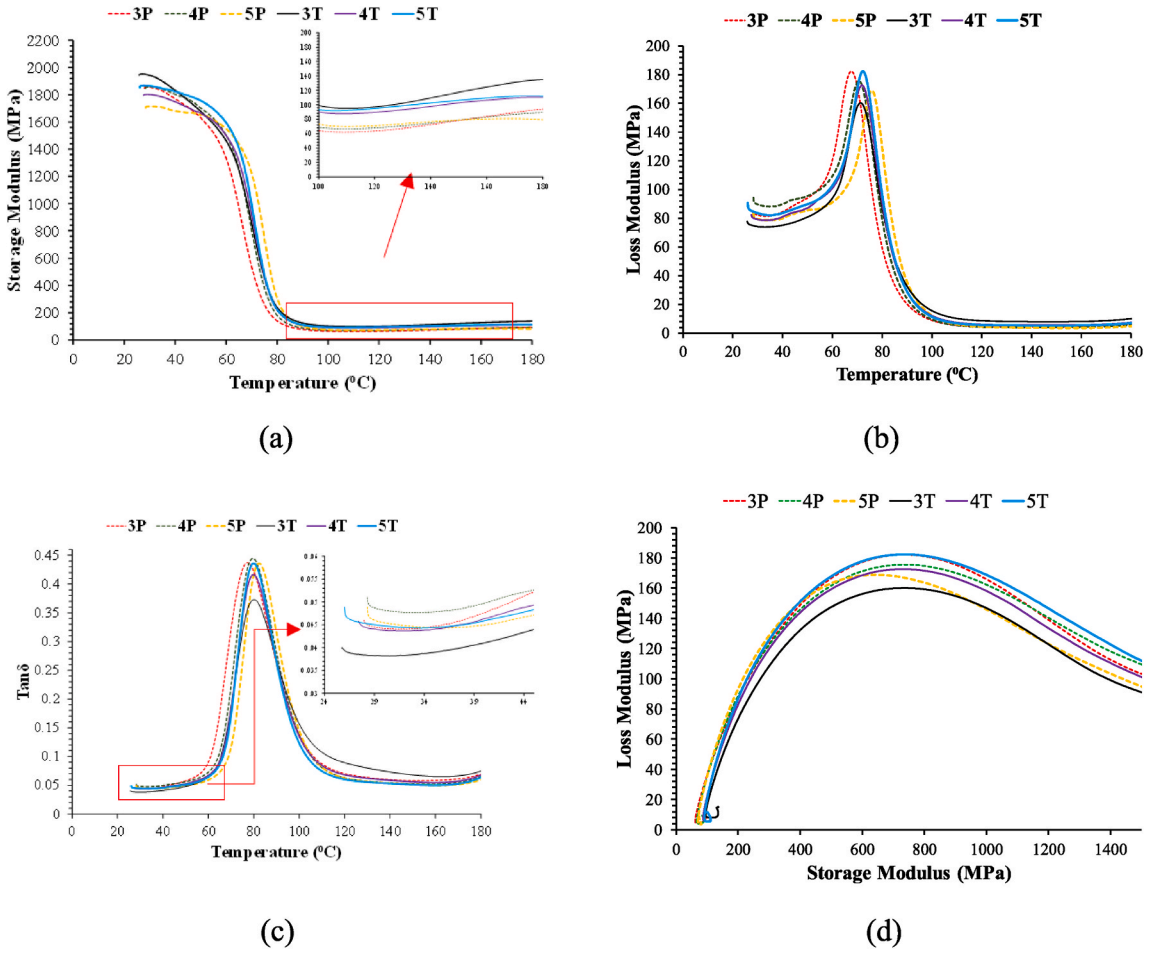

Fig. 7. DMA results as (**a**) Storage Modulus v/s Temperature; (**b**) Loss Modulus v/s Temperature; (**c**) Tanδ v/s Temperature; (**d**) Cole-Cole plot.

bonding sites to thickness [36]. This infers the dissipation of higher energy by 5T due to internal friction or molecular motion at the interface [49,50]. The area under the curve for both the composites has been the same, indicating the volume fraction of reinforcement maintained was constant.

3.3.3. Loss factor (tanδ)

A lower value of the loss factor indicates an elastic behavior and a higher value, damping [51]. In Fig. 7c, the damping factor has not changed for PWC inferring the stiffer properties of plain weave fabric. A soft fiber-matrix interface of PWC deduced from micrographs in Fig. 8 displays fiber pullouts with the presence of resin on surface, implying their damping behavior [52]. TWC with a higher float length and fewer interlacements, have shown an increase in tanδ peak from 3T to 5T. The micrographs in Fig. 8, indicated an improvement in wettability and fiber breakages for TWC, thus inferring the shift in elastic to damping behavior [36,53]. 5T has shown a higher value of storage and loss modulus, indicating a better damping property [50].

3.3.4. Cole-Cole plot

In Fig. 7d, PWC has shown an elliptical shape indicating a multiphase formation at the interphase, whereas TWC displayed a semi-circle, inferring a homogenous formation [54]. With increasing thickness, the peaks of TWC increased, indicating a rise in the homogenous percentage of material and it was higher for 5T. The overall results infer, thickness and weave pattern of composites have an influence on visco-elastic behavior and 5T has shown better damping properties.

3.4. Micrographs

The freeze fractured DMA specimens for PWC and TWC as observed under SEM are presented in Fig. 8a–f for different thicknesses. The amount of resin on the PWC was seen to be very poor compared to TWC inferring a higher amount of resin on the surface of fiber. Furthermore, tested specimens show loose filaments due to fiber pullouts in PWC, whereas in the TWC bundled failure occurred due to fiber breakages, indicating a higher fiber/matrix bonding ratio and better interface observed from Fig. 8b, d and 8e, respectively. The

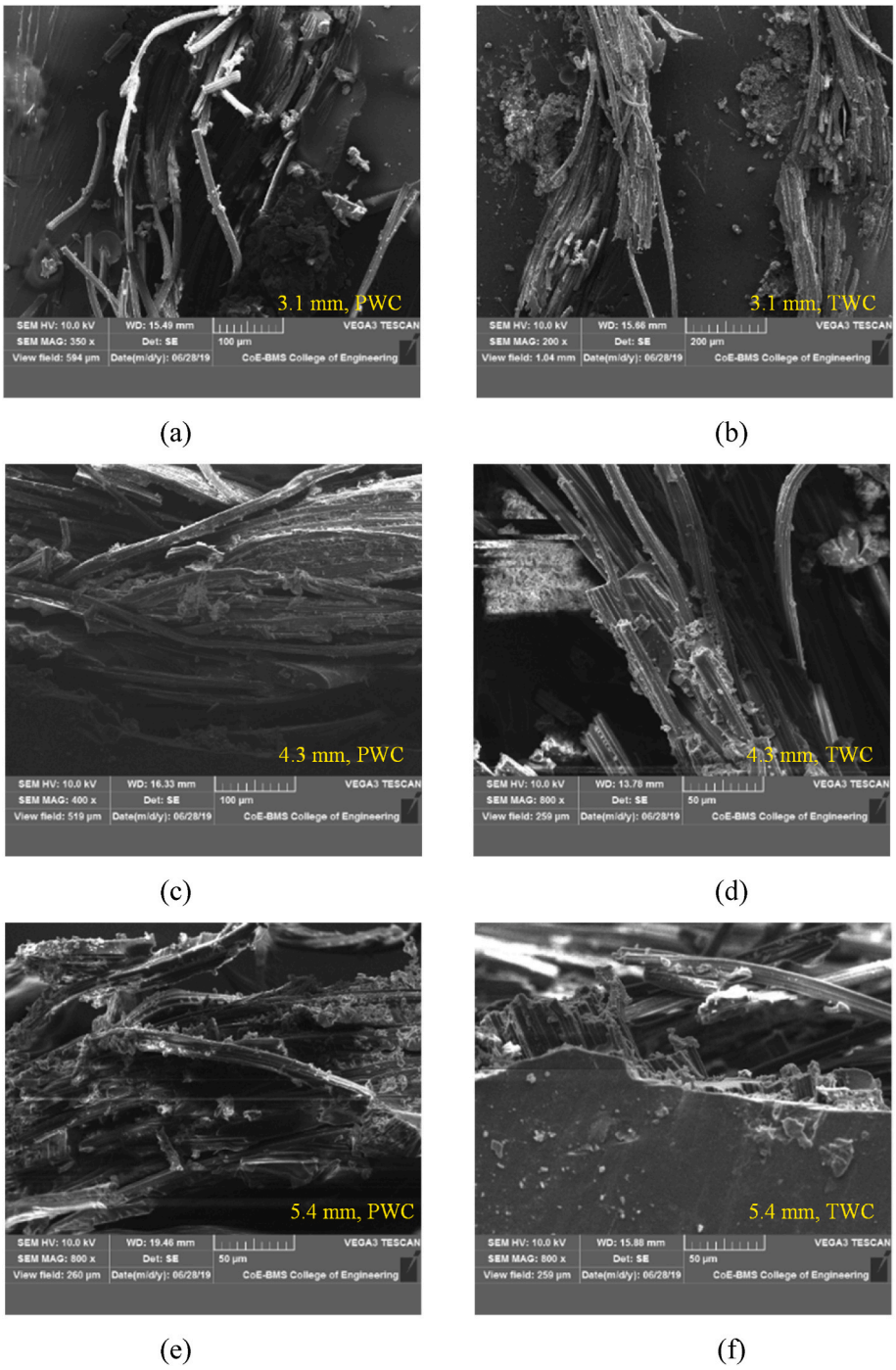

Fig. 8. SEM micrographs of specimens at (**a**) 3.1 mm, PWC (**b**) 3.1 mm, TWC, (**c**) 4.3 mm, PWC, (**d**) 4.3 mm, TWC, (**e**) 5.4 mm, PWC and (**f**) 5.4 mm, TWC.

Table 6
Croslink density determined in rubbery region.

Crosslink Density	3P = 0.0533	4P = 0.0574	5P = 0.0601	3T = 0.0817	4T = 0.0752	5T = 0.0793

increase in thickness also shows the increase in load-carrying capacity and better bonding in composites (Fig. 8a–f). The SEM images also indicate the poor bonding between the plain weave and the matrix as compared to the twill weave that has shown a good amount of resin on the surface of the fabric [36].

3.5. Water absorption

The results plotted on graphs display the notations as 'S'- salt water and 'D'-distilled water. The hydroxyl groups present in the composites develop a new hydrogen bonding with water molecules as the water infuses through (a) micro-capillary units known as micro-fibrils, (b) micro-gaps between polymer chains, and (c) micro-cracks formed during processing, which leads to swelling [55]. PWC and TWC have shown a reduction in water absorption with increasing thickness as observed in Table 5, whereas few works have shown increasing behavior [56,57]. The crossover points in plain weave fabrics were higher than the twill weave, this led to the formation of micro-cracks at these points due to swelling after water infusion. These micro-cracks paved way for more amount of water absorption by capillary action than TWC. Because TWC possesses fewer interlacements, better wettability as observed in micrographs Fig. 8 and the homogenous formation in Cole-Cole plot Fig. 7d [58]. In Fig. 9, a linear rate of absorption was observed after 4 days, resembling Fickian diffusion behavior till attaining saturation [59]. In Fig. 9a–b, 5P showed a 35% reduction in water absorption compared to 3P in D-solution and 39% in S-solution, after a week. Similarly, 5T showed a 25% reduction in D-solution and 23% in S-solution, compared to 3T. 3T showed an improvement of 21.4% and 4T showed 18.4% compared to 3P and 4P respectively, in resisting the absorption. At 5.4 mm thickness, PWC and TWC have shown similar resistance to absorption in both solutions. This was due to better bonding as observed from the micrographs in Fig. 8, which displayed fiber breakages and wettability [36]. In Fig. 9c–d, we can observe the absorption of distilled water was higher compared to salt, which is due to the presence of salt content that hinders the absorption in both the composites [60].

3.6. Flammability

The graph plotted in Fig. 10, shows the minimal impact of the weave pattern on the flammability of composites. An increase in

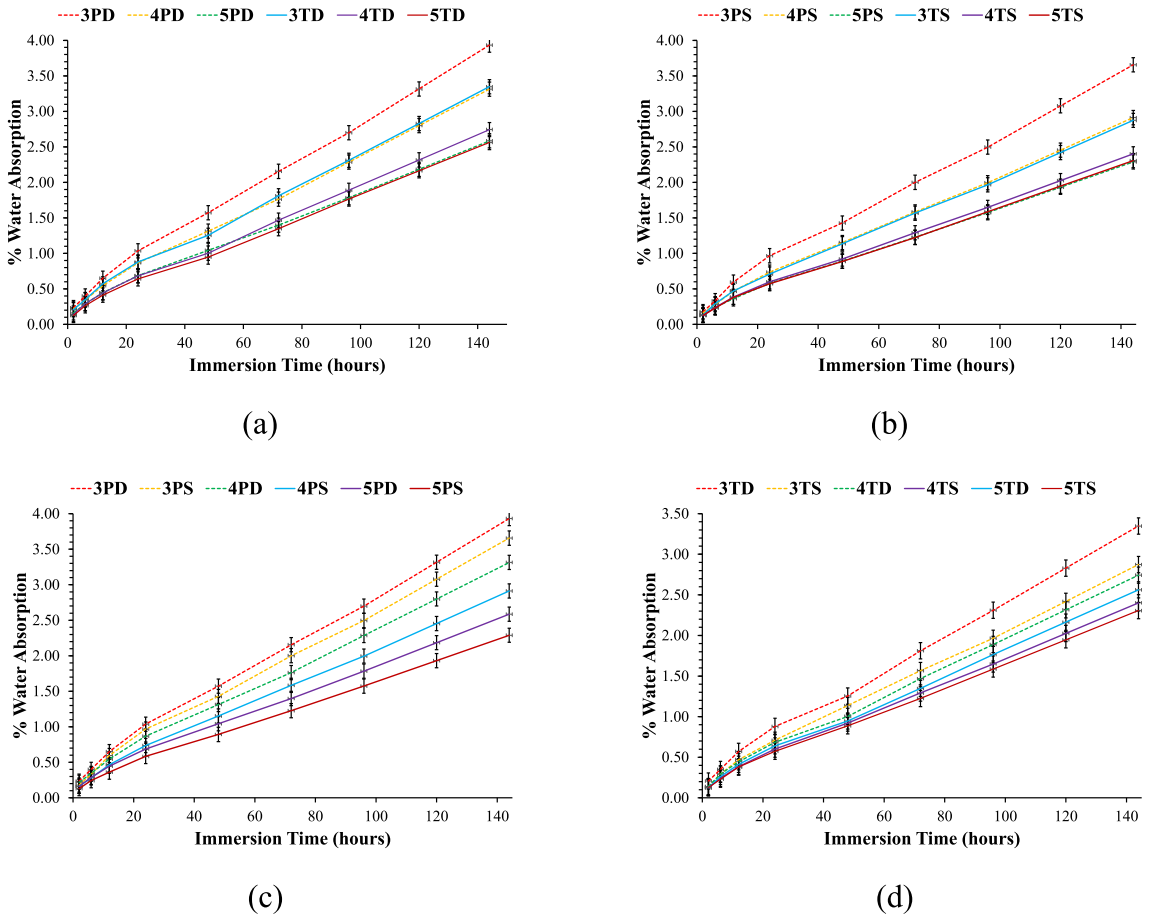

Fig. 9. (**a**) Distilled water (D); (**b**) Salt water (S;) (**c**) PWC; (**d**) TWC.

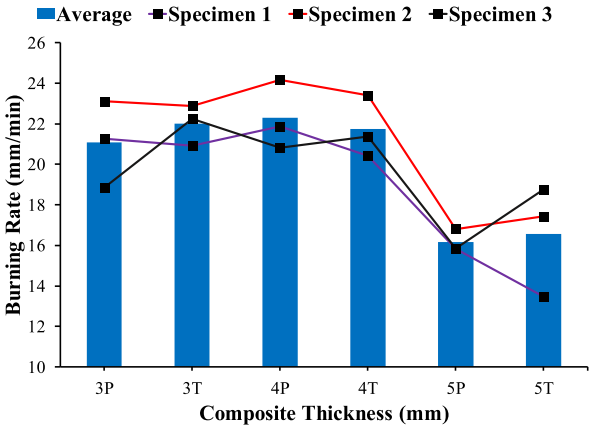

Fig. 10. Horizontal burning test of plain and twill weave composites.

thickness increased the time for ignition by reducing the burning rate [61]. SEM micrographs observed in Fig. 8 display the increase in wettability of composites from 3.1 mm to 5.4 mm thickness. This wettability of composites reduced the burning rate at 5.4 mm thickness by 30% compared to 3.1 mm as observed in Table 4 [36,62].

4. Conclusions

The use of lightweight materials as a substitute for synthetic reinforcements showed the composite performance at coupon level as a function of weave design and thickness. The results conveyed that the lesser interlacements in TWC showed an improvement in T_g and capacity to absorb the heat at higher thickness. A lower tanδ value in DMA indicates the material's capacity to store energy, whereas a higher number indicates energy dissipation. TWC's demonstrated better storing of energies at lower thickness and dissipates the energy at higher thickness implying that the area under the curve determined the amount of molecular mobility occurring to achieve damping, which was greater. TWC, which originally displayed resistance to absorption rate compared to PWC, saturated over time due, according to Fickians' behaviour. The weaving pattern had no influence on flammability, but the wettability and thickness of the composite reduced it.

Submission declaration and verification

The authors would like to confirm that work illustrated has not been published before and it is not under consideration for publication anywhere else.

Author contribution statement

Gangadhar M Kanaginahal: Conceived and designed the experiments; Contributed reagents, materials, analysis tools or data; Wrote the paper.

Suresh Hebbar: Conceived and designed the experiments; Contributed reagents, materials, analysis tools or data.

Kiran Shahapurkar: Conceived and designed the experiments; Analyzed and interpreted the data; Wrote the paper.

Mohammed A. Alamir, Vineet Tirth: Performed the experiments.

Ibrahim M. Alarifi: Analyzed and interpreted the data.

Mika Sillanpaa: Contributed reagents, materials, analysis tools or data.

H C Ananda Murthy: Analyzed and interpreted the data; Wrote the paper.

Funding statement

The Authors extend their thanks to the Deanship of Scientific Research at King Khalid University for funding this work through the small research groups under grant number RGP. 2/246/43.

Data availability statement

The data used to support the findings of this study are included within the article.

Declaration of interest's statement

The authors declare no competing interests.

Acknowledgments

The authors would like to express their gratitude to the Department of Mechanical Engineering, N.I.T.K., Surathkal.

References

[1] A. Partanen, M. Carus, Wood and natural fiber composites current trend in consumer goods and automotive parts, Reinforc Plast 60 (2016) 170–173, https://doi.org/10.1016/J.REPL.2016.01.004.
[2] T. Väisänen, O. Das, L. Tomppo, A review on new bio-based constituents for natural fiber-polymer composites, J. Clean. Prod. 149 (2017) 582–596, https://doi.org/10.1016/J.JCLEPRO.2017.02.132.
[3] L. Mohammed, M.N.M. Ansari, G. Pua, et al., A review on natural fiber reinforced polymer composite and its applications, Int. J. Polym. Sci. 1–15 (2015), https://doi.org/10.1155/2015/243947, 2015.
[4] T. Gurunathan, S. Mohanty, S.K. Nayak, A review of the recent developments in biocomposites based on natural fibres and their application perspectives, Compos. Part A Appl Sci Manuf 77 (2015) 1–25, https://doi.org/10.1016/J.COMPOSITESA.2015.06.007.
[5] A. Javadian, I.F.C. Smith, D.E. Hebel, Application of sustainable bamboo-based composite reinforcement in structural-concrete beams: design and evaluation, Materials 13 (2020) 1–25, https://doi.org/10.3390/ma13030696.
[6] H. Zhong, Q. Shan, J. Zhang, et al., Flexural properties of steel-bamboo composite slabs in different connection methods, Adv. Civ. Eng. (2020) 1–10, https://doi.org/10.1155/2020/6639789, 2020.
[7] A. Muhammad, M.R. Rahman, S. Hamdan, K. Sanaullah, Recent developments in bamboo fiber-based composites: a review, Polym. Bull. 76 (2018) 1–28, https://doi.org/10.1007/s00289-018-2493-9.
[8] P. Van Der Lugt, J. Vogtländer, H. Brezet, et al., Bamboo, a Sustainable Solution for Western Europe Design Cases, LCAs and Land-Use, 2009.
[9] N.S. Ha, G. Lu, A review of recent research on bio-inspired structures and materials for energy absorption applications, Compos. B Eng. 181 (2019) 1–97, https://doi.org/10.1016/j.compositesb.2019.107496.
[10] M. Hu, C. Wang, C. Lu, et al., Investigation on the classified extraction of the bamboo fiber and its properties, J. Nat. Fibers 16 (2019) 1–14, https://doi.org/10.1080/15440478.2019.1599311.
[11] L. Osorio, E. Trujillo, F. Lens, et al., In-depth study of the microstructure of bamboo fibres and their relation to the mechanical properties, J. Reinforc. Plast. Compos. 37 (2018) 1–15, https://doi.org/10.1177/0731684418783055.
[12] R.F. Buson, L.F.L. Melo, M.N. Oliveira, et al., Physical and mechanical characterization of surface treated bamboo fibers, Sci. Technol. Mater. 30 (2018) 67–73, https://doi.org/10.1016/j.stmat.2018.03.002.
[13] T. Richmond, L. Lods, J. Dandurand, et al., Thermal and mechanical performances of bamboo strip, Mater. Res. Express 8 (2021) 1–11, https://doi.org/10.1088/2053-1591/abe060.
[14] J.-K. Huang, W.-B. Young, The mechanical, hygral, and interfacial strength of continuous bamboo fiber reinforced epoxy composites, Compos. B Eng. 166 (2019) 272–283, https://doi.org/10.1016/j.compositesb.2018.12.013.
[15] F. Wang, M. Lu, S. Zhou, et al., Effect of fiber surface modification on the interfacial adhesion and thermo-mechanical performance of unidirectional epoxy-based composites reinforced with bamboo fibers, Molecules 24 (2019) 1–14, https://doi.org/10.3390/molecules24152682.
[16] H.H. Chiu, W Bin Young, The longitudinal and transverse tensile properties of unidirectional and bidirectional bamboo fiber reinforced composites, Fibers Polym. 21 (2020) 2938–2948, https://doi.org/10.1007/s12221-020-0109-0.
[17] F. Wanderson Moreira Ribeiro, B. Lloyd Ryan Viana Kotzebue, J. Ribeiro Oliveira, et al., Thermal and mechanical analyses of biocomposites from cardanol-based polybenzoxazine and bamboo fibers, J. Therm. Anal. Calorim. 129 (2017) 281–289, https://doi.org/10.1007/s10973-017-6191-x.
[18] L. Lods, T. Richmond, J. Dandurand, et al., Thermal stability and mechanical behavior of technical bamboo fibers/bio-based polyamide composites, J. Therm. Anal. Calorim. 147 (2021) 1097–1106, https://doi.org/10.1007/s10973-020-10445-z.
[19] M. Yang, F. Wang, S. Zhou, et al., Thermal and mechanical performance of unidirectional composites from bamboo fibers with varying volume fractions, Polym. Compos. 40 (2019) 1–9, https://doi.org/10.1002/pc.25253.
[20] F. Wang, S. Zhou, M. Yang, et al., Thermo-mechanical performance of polylactide composites reinforced with alkali-treated bamboo fibers, Polymers 10 (2018) 1–14, https://doi.org/10.3390/polym10040401.
[21] F. Wang, M. Yang, S. Zhou, et al., Effect of fiber volume fraction on the thermal and mechanical behavior of polylactide-based composites incorporating bamboo fibers, J. Appl. Polym. Sci. 135 (2018) 1–9, https://doi.org/10.1002/app.46148.
[22] T.-C. Yang, T.-L. Wu, K.-C. Hung, et al., Mechanical properties and extended creep behavior of bamboo fiber reinforced recycled poly(lactic acid) composites using the time-temperature superposition principle, Construct. Build. Mater. 93 (2015) 558–563, https://doi.org/10.1016/j.conbuildmat.2015.06.038.
[23] C. Wang, L. Cai, S.Q. Shi, et al., Thermal and flammable properties of bamboo pulp fiber/high-density polyethylene composites: influence of preparation technology, nano Calcium carbonate and fiber content, Renew. Energy 134 (2019) 436–445, https://doi.org/10.1016/j.renene.2018.09.051.
[24] H. Judawisastra, R.D.R. Sitohang, M.S. Rosadi, Water absorption and tensile strength degradation of petung bamboo (dendrocalamus asper) fiber-reinforced polymeric composites, Mater. Res. Express 4 (2017) 1–8, https://doi.org/10.1088/2053-1591/aa8a0d.
[25] S.S. Chee, M. Jawaid, M.T.H. Sultan, et al., Thermomechanical and dynamic mechanical properties of bamboo/woven kenaf mat reinforced epoxy hybrid composites, Compos. B Eng. 163 (2019) 165–174, https://doi.org/10.1016/j.compositesb.2018.11.039.
[26] S.K. Lee, E.Y. Park, T.S. Park, S.K. An, Mechanical properties of PP/glass fiber/kenaf/bamboo fiber-reinforced hybrid composite, Fibers Polym. 22 (2021) 1460–1465, https://doi.org/10.1007/s12221-021-0358-6.
[27] W. Liu, T. Chen, Fei M. en, et al., Properties of natural fiber-reinforced biobased thermoset biocomposites: effects of fiber type and resin composition, Compos. B Eng. 171 (2019) 87–95, https://doi.org/10.1016/j.compositesb.2019.04.048.
[28] V. Mittal, R. Saini, S. Sinha, Natural fiber-mediated epoxy composites – a review, Compos. B Eng. 99 (2016) 425–435, https://doi.org/10.1016/J.COMPOSITESB.2016.06.051.
[29] N.Z.M. Zuhudi, R.J.T. Lin, K. Jayaraman, Flammability, thermal and dynamic mechanical properties of bamboo-glass hybrid composites, J. Thermoplast. Compos. Mater. 29 (2016) 1210–1228, https://doi.org/10.1177/0892705714563118.
[30] F. Lahuerta, R.P.L. Nijssen, F.P. Van Der Meer, L.J. Sluys, The influence of curing cycle and through thickness variability of properties in thick laminates, J. Compos. Mater. 51 (2017) 563–575, https://doi.org/10.1177/0021998316648758.
[31] F. Lahuerta, R.P.L. Nijssen, F.P. van der Meer, L.J. Sluys, Thickness scaled compression tests in unidirectional glass fibre reinforced composites in static and fatigue loading, Compos. Sci. Technol. 123 (2016) 115–124, https://doi.org/10.1016/j.compscitech.2015.12.008.
[32] C. Anand Chairman, S. Jayasathyakawin, S.P. Kumaresh Babu, M. Ravichandran, Mechanical properties of basalt fabric plain and twill weave reinforced epoxy composites, Mater. Today Proc. 46 (2019) 9480–9483, https://doi.org/10.1016/j.matpr.2020.03.240.
[33] A. Alavudeen, N. Rajini, S. Karthikeyan, et al., Mechanical properties of banana/kenaf fiber-reinforced hybrid polyester composites: effect of woven fabric and random orientation, Mater. Des. 66 (2015) 246–257, https://doi.org/10.1016/j.matdes.2014.10.067.
[34] R. Fangueiro, S. Rana, Natural Fibres: Advances in Science and Technology towards Industrial Applications, 2016.

[35] F. Lahuerta, THICKNESS EFFECT IN COMPOSITE LAMINATES IN STATIC AND FATIGUE LOADING, Universidad de Zaragoza, Spanje, 2016.
[36] G.M. Kanaginahal, H. Suresh Hebbar, S.M. Kulkarni, Influence of weave pattern and composite thickness on mechanical properties of bamboo/epoxy composites, Mater. Res. Express 6 (2019) 1–13, https://doi.org/10.1088/2053-1591/ab5a90.
[37] A. Porras, A. Maranon, Development and characterization of a laminate composite material from polylactic acid (PLA) and woven bamboo fabric, Compos. B Eng. 43 (2012) 2782–2788, https://doi.org/10.1016/J.COMPOSITESB.2012.04.039.
[38] J.C. dos Santos, R.L. Siqueira, L.M.G. Vieira, et al., Effects of Sodium carbonate on the performance of epoxy and polyester coir-reinforced composites, Polym. Test. 67 (2018) 533–544, https://doi.org/10.1016/J.POLYMERTESTING.2018.03.043.
[39] A.U. Md Shah, M.T. H Sultan, F. Cardona, et al., Thermal analysis of bamboo fibre and its composites, Bioresources 12 (2017) 2394–2406.
[40] P. Krishnan, Synthesis and characterization of cashew nut shell liquid (CNSL) matrix compositions for composites applications, in: International Conference on Natural Polymers, 2015, pp. 1–5.
[41] K. Zhang, F. Wang, W. Liang, et al., Thermal and mechanical properties of bamboo fiber reinforced epoxy composites, Polymers 10 (2018) 1–18, https://doi.org/10.3390/polym10060608.
[42] A.Q. Dayo, B. Gao, J. Wang, et al., Natural Hemp fiber reinforced polybenzoxazine composites: curing behavior, mechanical and thermal properties, Compos. Sci. Technol. 144 (2017) 114–124, https://doi.org/10.1016/J.COMPSCITECH.2017.03.024.
[43] J. Naveen, M. Jawaid, E.S. Zainudin, et al., Thermal degradation and viscoelastic properties of kevlar/cocos nucifera sheath reinforced epoxy hybrid composites, Compos. Struct. 219 (2019) 194–202, https://doi.org/10.1016/J.COMPSTRUCT.2019.03.079.
[44] C. Wang, S. Ying, A novel strategy for the preparation of bamboo fiber reinforced polypropylene composites, Fibers Polym. 15 (2014) 117–125, https://doi.org/10.1007/s12221-014-0117-z.
[45] M.J.M. Ridzuan, M.S.A. Majid, M. Afendi, et al., Thermal behaviour and dynamic mechanical analysis of pennisetum purpureum/glass-reinforced epoxy hybrid composites, Compos. Struct. 152 (2016) 850–859, https://doi.org/10.1016/J.COMPSTRUCT.2016.06.026.
[46] J. Zhang, S. Xu, Effect of chain length of cardanol-based phenalkamines on mechanical properties of air-dried and heat-cured epoxies, Mater. Express 9 (2019) 337–343, https://doi.org/10.1166/mex.2019.1498.
[47] F.X. Espinach, S. Boufi, M. Delgado-Aguilar, et al., Composites from poly(lactic acid) and bleached chemical fibres: thermal properties, Compos. B Eng. 134 (2018) 169–176, https://doi.org/10.1016/J.COMPOSITESB.2017.09.055.
[48] V.S. Sreenivasan, N. Rajini, A. Alavudeen, V. Arumugaprabu, Dynamic mechanical and thermo-gravimetric analysis of sansevieria cylindrica/polyester composite: effect of fiber length, fiber loading and chemical treatment, Compos. B Eng. 69 (2015) 76–86, https://doi.org/10.1016/J.COMPOSITESB.2014.09.025.
[49] N. Kumar, D. Das, Fibrous biocomposites from nettle (girardinia diversifolia) and poly(lactic acid) fibers for automotive dashboard panel application, Compos. B Eng. 130 (2017) 54–63, https://doi.org/10.1016/J.COMPOSITESB.2017.07.059.
[50] Y.S. Song, J.T. Lee, D.S. Ji, et al., Viscoelastic and thermal behavior of woven Hemp fiber reinforced poly(lactic acid) composites, Compos. B Eng. 43 (2012) 856–860, https://doi.org/10.1016/j.compositesb.2011.10.021.
[51] S. Kumar, K. Bhabani • Satapathy, A. Patnaik, Viscoelastic interpretations of erosion performance of short aramid fibre reinforced vinyl ester resin composites, J. Mater. Sci. 46 (2011) 7489–7500, https://doi.org/10.1007/s10853-011-5719-x.
[52] V. Fiore, L. Calabrese, Effect of stacking sequence and Sodium bicarbonate treatment on quasi-static and dynamic mechanical properties of flax/jute epoxy-based composites, Materials 12 (2019) 1–18, https://doi.org/10.3390/ma12091363.
[53] M. Rajesh, S.P. Singh, J. Pitchaimani, Mechanical behavior of woven natural fiber fabric composites: effect of weaving architecture, intra-ply hybridization and stacking sequence of fabrics, J. Ind. Textil. 47 (2018) 938–959, https://doi.org/10.1177/1528083716679157.
[54] V. Panwar, K. Pal, An optimal reduction technique for rGO/ABS composites having high-end dynamic properties based on cole-cole plot, degree of entanglement and C-factor, Compos. B Eng. 114 (2017) 46–57, https://doi.org/10.1016/j.compositesb.2017.01.066.
[55] M. Chandrasekaran, M.R. Ishak, S.M. Sapuan, et al., A review on the characterisation of natural fibers and their composites after alkali treatment and water absorption, Plast., Rubber Compos. 46 (2017) 119–136, https://doi.org/10.1080/14658011.2017.1298550.
[56] K. Muktha, B.S. Keerthi Gowda, Investigation of water absorption and fire resistance of untreated banana fibre reinforced polyester composites, Mater. Today Proc. 4 (2017) 8307–8312, https://doi.org/10.1016/j.matpr.2017.07.173.
[57] R.K. Kejariwal, B.S. Keerthi Gowda, Flammability and moisture absorption behavior of sisal-polyester composites, Mater. Today Proc. 4 (2017) 8040–8044, https://doi.org/10.1016/J.MATPR.2017.07.142.
[58] Z.N. Azwa, B.F. Yousif, A.C. Manalo, W. Karunasena, A review on the degradability of polymeric composites based on natural fibres, Mater. Des. 47 (2013) 424–442, https://doi.org/10.1016/J.MATDES.2012.11.025.
[59] N. Cuinat-Guerraz, M.-J. Dumont, P. Hubert, Environmental resistance of flax/bio-based epoxy and flax/polyurethane composites manufactured by resin transfer moulding, Compos. Part A Appl Sci Manuf 88 (2016) 140–147, https://doi.org/10.1016/J.COMPOSITESA.2016.05.018.
[60] H. Jena, A.K. Pradhan, M.K. Pandit, Studies on water absorption behaviour of bamboo-epoxy composite filled with cenosphere, J. Reinforc. Plast. Compos. 33 (2014) 1059–1068, https://doi.org/10.1177/0731684414523325.
[61] T. Fateh, C. Kahanji, P. Joseph, T. Rogaume, A study of the effect of thickness on the thermal degradation and flammability characteristics of some composite materials using a cone calorimeter, J. Fire Sci. 35 (2017) 547–564, https://doi.org/10.1177/0734904117713690.
[62] M.S. Salim, A. Rasyid, M.A. Abdullah, et al., Mechanical, thermal and flammability properties of nonwoven kenaf reinforced acrylic based polyester composites: effect of water glass treatment, in: IOP Conference Series: Materials Science and Engineering PAPER, 2018, pp. 1–12.